LIMNOLOGY AND OCEANOGRAPHY
Letters

ASLO
Open Access

Limnology and Oceanography Letters 2022

doi: 10.1002/lol2.10215

SPECIAL ISSUE-LETTER

Impact of salinization on lake stratification and spring mixing

Robert Ladwig ,* *Linnea A. Rock* , *Hilary A. Dugan*
Center for Limnology, University of Wisconsin-Madison, Madison, Wisconsin

Scientific Significance Statement

Around the world, freshwater lakes are increasing in salinity due to salt pollution. High salt concentrations can harm freshwater organisms but also can stabilize lake water columns because saline water is denser than freshwater. In a worst case scenario, salinization can prevent the ecologically important spring turnover event of the water column. Using multiple approaches, we found that increased winter salt loading will delay spring turnover, prolong summer stratification, and increase water column stability during spring, summer, and winter in north temperate lakes.

Abstract

Anthropogenic freshwater salinization affects thousands of lakes worldwide, and yet little is known about how salt loading may shift timing of lake stratification and spring mixing in dimictic lakes. Here, we investigate the impact of salinization on mixing in Lakes Mendota and Monona, Wisconsin, by deploying under-ice buoys to record salinity gradients, using an analytical approach to quantify salinity thresholds that prevent spring mixing, and running an ensemble of vertical one-dimensional hydrodynamic lake models (GLM, GOTM, and Simstrat) to investigate the long-term impact of winter salt loading on mixing and stratification. We found that spring salinity gradients between surface and bottom waters persist up to a month after ice-off, and that theory predicts a salinity gradient of 1.3–1.4 g kg^{-1} would prevent spring mixing. Numerical models project that salt loading delays spring mixing and increases water column stability, with ramifications for oxygenation of bottom waters, biogeochemistry, and lake habitability.

Humans are heavily altering the natural concentrations of salt in inland waters, through agricultural runoff, wastewater treatment discharge, and road salt application (Novotny et al. 2008; Kelly et al. 2010; Richards et al. 2010; Dugan and Rock 2021). At the regional to continental scale, salinization is a widespread environmental issue, as it is predicted to affect

*Correspondence: rladwig2@wisc.edu

Associate editor: Alison Derry

Author Contribution Statement: RL and HD designed the study. RL conducted the analytical and numerical modeling. LR conducted the field monitoring. RL, HD, and LR analyzed the data and co-wrote the manuscript.

Data Availability Statement: All driver, model, and observed data as well as scripts to process data into quantitative metrics and figures are archived and accessible at Zenodo: https://doi.org/10.5281/zenodo.5504319 (Ladwig et al. 2021b). High-frequency buoy data of electrical conductivity and water temperature since 2019 are available at https://doi.org/10.6073/pasta/1bef2de0650bdc9e90a422b61aaa59e5 (Rock and Dugan 2021). Historical chloride data for Lake Mendota and Monona are available at https://doi.org/10.6073/pasta/fbc6e00b0397af00345d5976cfc782be and https://doi.org/10.6073/pasta/a457e305538a0d8e669b58bb6f35721f. Lake shapefiles and bathymetry are available at https://doi.org/10.6073/pasta/bfc7fcc762572c72e2d2d35cab1d7662 and https://doi.org/10.6073/pasta/7b0a93bd469d6072cc22ec3355483df8.

Additional Supporting Information may be found in the online version of this article.

over 7000 lakes in the US Midwest and Northeast (Dugan et al. 2020). Salinization of freshwater environments can harm biological function (Corsi et al. 2010; Van Meter and Swan 2014), trigger trophic cascades (Hintz et al. 2017), and inhibit plant growth (EPA 1988), and high chloride concentrations can lead to potential corrosivity of water distribution systems, which can release lead and copper into drinking water supplies (Stets et al. 2017).

A less studied aspect of lake salinization is the potential for salt to affect lake stratification and mixing. The density profile of a lake water column is the determinant of mixing dynamics (Boehrer and Schultze 2008). In freshwater lakes, temperature effects on water density are typically the dominant control on lake stratification. However, the addition of salt ions to freshwater increases water density, and salinity quickly becomes a much stronger regulator of water density than temperature. For instance, the difference in density between freshwater at 10°C and 20°C is 1.496 kg m^{-3}; approximately the same difference as 0–2 g kg^{-1} salinity at 20°C and 1 dbar, as calculated with the seawater equation of state (Millero and Poisson 1981).

The accumulation of anthropogenic salts in a lake can increase density gradients in the water column and lead to delayed, diminished, or disrupted lake mixing. In Michigan, 12-m deep Woods Lake transitioned from holomixis to meromixis due to sustained road salt inputs (Koretsky et al. 2012; Sibert et al. 2015), which led to persistent bottom water anoxia. Hypolimnetic chloride concentrations reached 290 mg L^{-1}, and a density difference of 0.3 kg m^{-3} between the lake surface and bottom prevented turnover (comparable to the water density difference resulting from a temperature difference of 15 to 17°C without any salinity). A similar phenomenon was seen in 23-m deep Irondequoit Bay in Lake Ontario (Pesacreta and Makarewicz 1982; Bubeck and Burton 1989). Saline runoff led to spring hypolimnetic chloride concentrations of 360–410 mg L^{-1}, which prevented spring mixing. In Austria, for decades, industrial saline effluent was discharged into the epilimnion of Traunsee, 191-m deep alpine lake (Ficker et al. 2018), but there were only two distinct periods of meromixis: (1) When effluent was discharged directly into the hypolimnion and the density gradient was >0.5 kg m^{-3} and (2) When industrial discharges were stopped, the eplimnion freshened and deepened, and although density differences became <0.1 kg m^{-3}, the established meromixis, which began during the recovery from salinization, persisted. The maximum chloride concentrations were 170 mg L^{-1}.

Conceptually, we are interested in the effects of saline winter runoff on lake stratification and spring mixing (Fig. 1). In watersheds where road salt is applied in the winter, melt events may cause saline runoff to intrude into the lake water column and dissolved salts to accumulate at the lake bottom. Any increase in hypolimnetic salinity would increase the water column density gradient compared to conditions without salt inputs. Following ice-off, the greater the vertical density gradient, the greater the external kinetic forces required to mix the water column. Therefore, any salinity gradient can potentially delay spring mixing. In an extreme scenario, changing the density of lake water due to anthropogenic salt inputs can shift a normally dimictic lake to meromictic or monomictic. Amixis can have serious cascading consequences on lake biogeochemistry and lake habitat, as bottom waters become anoxic due to lack of oxygenation from surface water renewal (Straile et al. 2003). Apart from case studies that have documented a change in lake mixing regimes, there has been little analytical or mechanistic modeling of the impact of rising salt concentrations on freshwater lake mixing dynamics. Here, we quantify the theoretical salt threshold that would prevent spring turnover in two urban Wisconsin lakes. Further, we use three vertical one-dimensional hydrodynamic lake models (GLM, GOTM, and Simstrat) to investigate the impact of salt loading on mixing and stratification. Lake hydrodynamic modeling provides an insight into thresholds at which salt concentrations impact lake physics and supports guidelines for managing salt inputs.

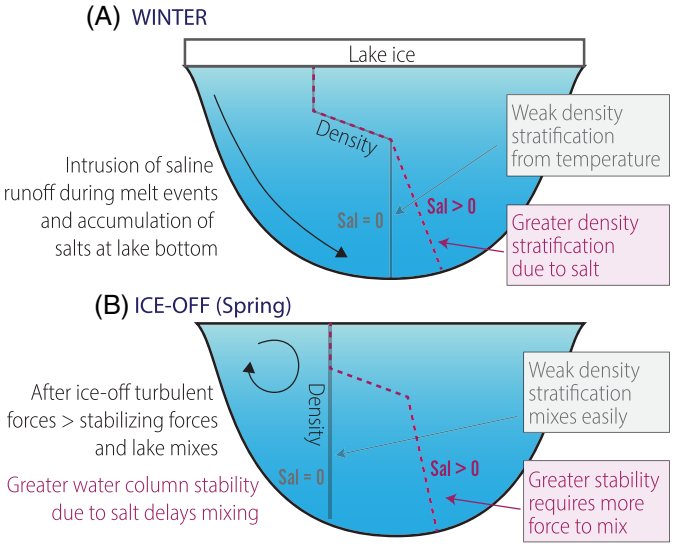

Fig 1. Conceptual sketch of saltwater intrusion from runoffs accumulating at lake bottom and potentially delaying spring turnover. (**A**): During quit ice conditions, higher salinity runoff from the watershed entrains into the lake and accumulates at the bottom increasing the vertical density gradient. (**B**): After ice-off, external kinetic forces mix the lake water column. Here, the established density gradient caused by the accumulation of salt at lake bottom can potentially delay timing and duration of vertical mixing compared to conditions without accumulation of salt at the lake bottom.

Methods

Study lakes

We use Lake Mendota and Lake Monona, dimictic lakes in southern Wisconsin, to investigate the impact of salinization

on lake stratification (see Table S1 for lake characteristics). Both lakes have been increasing in salinity over the past 80 yr (Fig. 2), and in 2021, chloride concentrations were ~50 mg L^{-1} in Mendota and 80 mg L^{-1} in Monona. The highest recorded chloride concentrations (up to 373 mg L^{-1}) are always in the bottom samples (20 m) of Lake Monona in February/March when the lake is ice covered (Fig. S1) (NTL-LTER 2020).

In 2019, two in-situ HOBO electrical conductivity (EC) loggers were deployed in each lake on under-ice buoys and retrieved after ice-off (Rock and Dugan 2021). In each lake, the buoy string held loggers at approximately 1 m below the surface and 1 m from the lake bottom. The Lake Mendota buoy was lost in 2021, so no data were available for winter 2020–2021. Wind speed data were obtained from NOAA station USWOOO14837.

Modeling approach

We explore the effects of salt loading on lake stratification and mixing dynamics in Mendota and Monona under (a) idealized conditions in an analytical approach and (b) pseudo-field conditions in model space (Fig. 2B,C). In the analytical approach, we quantify the amount of salt needed to induce stabilizing conditions during spring turnover. To check this theoretical threshold under field conditions, we apply an ensemble of vertical 1D hydrodynamic lake models to investigate how mixing and stratification dynamics change under different salt loading scenarios in Lake Mendota and Monona from 1995 to 2015.

Analytical approach

Our analytical solution aims to quantify the hypolimnetic salinity threshold that will establish stabilizing conditions.

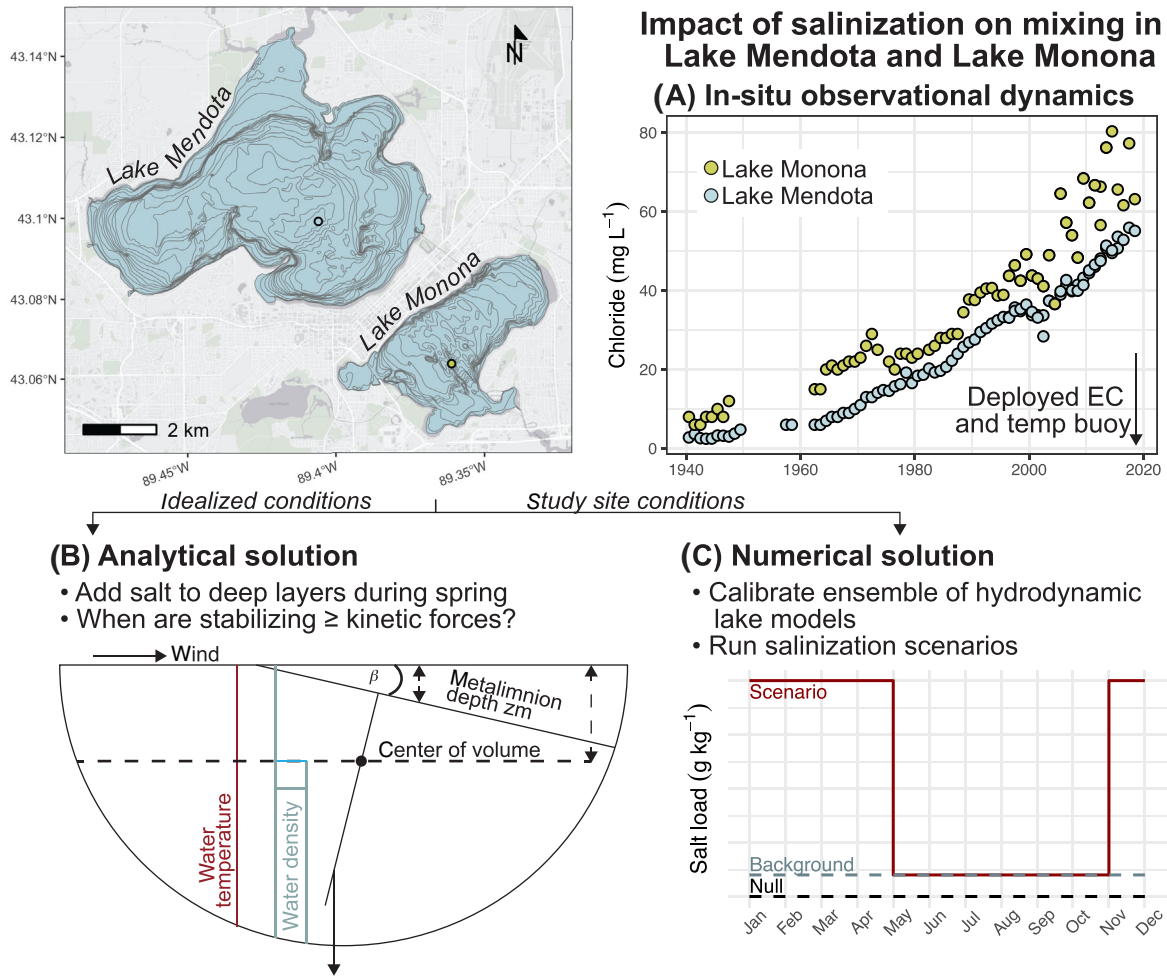

Fig 2. Conceptual framework to quantify the impact of salinization on lake spring mixing and stratification in 25-m deep Lake Mendota and 22-m deep Lake Monona, Wisconsin, using a three-tiered holistic approach: (**A**) deploy under-ice instrumentation to capture conductivity gradients throughout the winter and spring. Sampling and buoy sites denoted by circles on the bathymetric maps. (**B**) Analytically quantifying a critical salt load threshold that would prevent the lakes from experiencing spring turnover; and (**C**) use an ensemble of hydrodynamic lake models to simulate different salt load scenarios and quantify changes in lake stability.

For idealized cases of Mendota and Monona, we assume spring conditions to have a uniform vertical water temperature of 8°C and salinity of 0 g kg^{-1}, as well as a mean wind speed of 4.6 m s^{-1}. For each lake site, we use the respective hypsographies (area over depth relationships). We quantify the ratio of stabilizing to kinetic forces, or alternatively the mass moment to the wind moment, by using the Lake Number, *LN*, concept (Imberger and Patterson 1989) (further applied e.g., in Robertson and Imberger (1994); Lindenschmidt and Chorus (1998):

$$LN = \frac{g*\left(\mathrm{St}*\frac{A_0}{g}\right)*\beta}{\rho_{\mathrm{bottom}}*u_*^2*A_0*z_v} \quad (1)$$

in which St is the Schmidt stability, which quantifies the amount of external energy needed to mix the entire water column (which equals the potential energy stored in the water column) (J m^{-2}), β is the angle of the metalimnion surface to the lake bottom (dimensionless), ρ is water density (here, ρ_{bottom} represents density of the bottom layer) (kg m^{-3}), u_* is the wind friction velocity (m s^{-1}), A_0 is the lake surface area (m^2), and z_v is the center of volume depth (m). The Schmidt stability, St, can be quantified as:

$$\mathrm{St} = \frac{g}{A_0}*\int_0^{z_{\max}}(z - z_v)*A_z*\rho_z dz \quad (2)$$

here g is gravitational acceleration (m s^{-2}), z is the depth referenced from the water surface (m) (Idso 1973; Read et al. 2011). Please note that the Schmidt stability in Eq. 1 is multiplied by $g*\frac{A_0}{g}$ to achieve the potential energy in units of J. β can be approximated as:

$$\beta = \frac{z_m}{\sqrt{A_0}} \quad (3)$$

where z_m is the depth of the thermocline. The depth of the center of volume, z_v, is:

$$z_v = \frac{\int_0^{z_{\max}} z\rho_z A_z dz}{\int_0^{z_{\max}} \rho_z A_z dz} \quad (4)$$

We can estimate the friction velocity due to wind shear by:

$$u_*^2 = \frac{\rho_{\mathrm{air}}}{\rho_{\mathrm{surf}}}*C_D*U_{10}^2. \quad (5)$$

where ρ_{air} is the air density (kg m^{-3}), ρ_{surf} is the water density of the surface layer (kg m^{-3}), C_D is a drag coefficient (–), and U_{10} is the measured wind velocity at 10 m above the surface (m s^{-1}).

We quantify the salinity threshold (S_{crit}) that would result in a balance of stabilizing to kinetic forces as:

$$S_{\mathrm{crit}} \rightarrow g*\left(\mathrm{St}*\frac{A_0}{g}\right)*z_m = \rho_{\mathrm{bottom}}*u_*^2*A_0^{3/2}*z_v \quad (6)$$

This is the critical amount of salt that will – theoretically – result in amixis during spring. Note that we theoretically add a uniform salt amount only to the layers below the center of volume depth z_v of each lake without changing the heat content of the bottom layer (Fig. 2B). The density of water as a function of temperature and salinity was calculated according to Millero and Poisson (1981). S_{crit} was quantified in R using **`rLakeAnalyzer`** (Read et al. 2011) to calculate the Lake Number, and the Nelder–Mead optimization routine to derive the state when $S_{\mathrm{crit}} \rightarrow LN = 1 = g*\left(\mathrm{St}*\frac{A_0}{g}\right)*z_m = \rho_{\mathrm{bottom}}*u_*^2*A_0^{3/2}*z_v$.

Numerical approach

We used process-based modeling to further investigate how Mendota and Monona would be affected by varying salt loads under dynamic conditions. We apply the **`LakeEnsemblR`**-package (Moore et al. 2021) to run an ensemble of three vertical 1D hydrodynamic lake models, GLM v.3.1.0 (Hipsey et al. 2019), GOTM v.5.4.0-lake (Burchard et al. 1999; 2006) and Simstrat v.2.4.1 (Goudsmit et al. 2002; Gaudard et al. 2019). Although all of these models compute vertical transport via a form of turbulence closure scheme, the models differ regarding their hydrodynamic computations of vertical heat transport and entrainment dynamics.

Each model was initiated using the same initial conditions and driver data, and run at an hourly time-step. Inflow discharges and inlet water temperature into Lake Mendota were taken from the calibrated lake catchment model PIHM for the upper Yahara watershed (Qu and Duffy 2007; Ladwig et al. 2021*a*). The inflow into Lake Monona was taken from PIHM's calibrated Lake Mendota outflow. Inflow temperatures into Lake Monona were taken as the simulated surface water temperatures of the null scenario of Lake Mendota. Meteorological driver data (short-wave and long-wave radiation, air temperature, relative humidity, wind speed, precipitation) were derived from the second phase of the North American Land Data Assimilation System (Xia et al. 2012) with 1/8$^{\mathrm{th}}$-degree spacing grid cells centered at Lake Mendota. Observed water temperature data for model calibration were obtained from NTL-LTER (Magnuson et al. 2020).

Model outputs were saved on a daily time step. We ran a split-sample calibration for each model using 1995–2010 for calibrating model-specific parameters to improve the fit between observed and simulated water temperature data, and 2011–2015 for validating the achieved fit. For calibration, we used a Latin Hypercube Sampling approach with 5000 iterations randomly sampling model-specific parameters between given constraints. For each lake model, we calibrated multipliers for wind speed and short-wave radiation fluxes as well as model-specific parameters (see Table S2 for an overview). Salt loads were set to zero during the calibration and validation. We quantified model fits using the mean average error

(MAE), the root-mean square error (RMSE) and the Nash-Sutcliffe coefficient of efficiency (NSE) between simulated and observed water temperature data.

We ran the ensemble of lake models on the full time period (1995–2015) with varying inflow concentrations of salt (in total 13 scenarios):

- Null (*null*): Salt loads set to zero
- Background (BG): Constant salt load of 0.1 g kg^{-1} every day
- Winter salt scenarios: Constant salt load of 0.1 g kg^{-1} and independent scenarios where winter salt loads (December to April) in the river inflow were set to either 0.5, 1, 1.5, 2, 2.5, 3, 3.5, 4, 4.5, 5, or 10 g kg^{-1}

We averaged water temperature, salinity, density and ice thickness outputs from all models into mean ensemble values. Vertical gradients for water temperature and density were quantified using the difference between depths of 20 and 2 m from the surface. We quantified the first mixing day as the first day of the year when water density gradient was below 0.1 kg/m^3, water temperature gradient below 1°C, and ice thickness was zero [Correction added on 17 October 2021, after first online publication: The units of water density gradient in this sentence were modified]. The summer stratification period was quantified as the complete period of time when the 7-day moving average of water density gradient was above 0.1 kg/m^3 (Gray et al. 2020; Wilson et al. 2020), the water temperature gradient was above 1°C (Engelhardt and Kirillin 2014), ice thickness was zero, and Schmidt Stability was above zero [Correction added on 17 October 2021, after first online publication: The units of water density gradient in this sentence were modified]. The ice-covered period was quantified as the total duration of days with ice thickness > zero. The Lake Number (*LN*) was calculated using Eq. 1. To inspect changes across scenarios, we normalized the results from the scenarios by subtracting scenario-specific outputs from the output of the null run.

Results

In-situ spring mixing dynamics

Field data from Lake Mendota suggest that salt is entrained into the deep-water layers slightly after winter stratification is established (early-January when surface and bottom water temperature diverge). The EC gradient increases to about 200 μS cm^{-1} between deep and surface layers, which is equivalent to a salinity gradient of ~0.110 g kg^{-1} (Fig. 3A). The EC gradient diminishes strongly after ice breakup in late-March and becomes zero in April 2020.

In Lake Monona, the EC gradient is larger (500–700 μS cm^{-1}, equivalent to salinity ~0.27–0.38 g kg^{-1}) between bottom and surface layers and establishes immediately after ice formation (Fig. 3B). The elevated EC gradient in Monona is consistent with observations of increased chloride in the bottom waters under-ice (Fig. S1). Interestingly, in both lakes

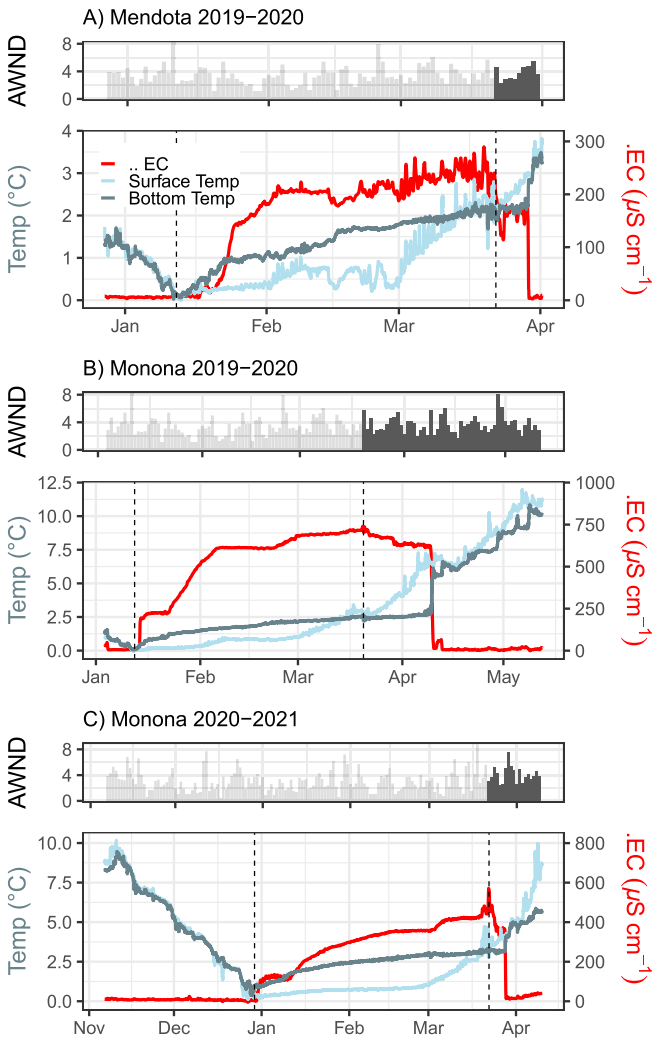

Fig 3. Winter to spring dynamics of the electrical conductivity gradient between surface and deep waters as well as surface and bottom water temperature time series highlighting the intrusion of saline water into the lakes Mendota and Monona. Upper panels show average daily wind speed (AWND m s^{-1}) taken at the nearby Dane County Regional Airport. Data prior to ice-off is grayed out. Lower panels show surface water temperature (at 2 m depth, light blue) and bottom (at 23.5 m depth in Mendota and 20 m in Monona, dark blue) water temperatures in the lakes over the winter/spring of 2019–2020 and 2020–2021. The red line shows the difference in specific conductance (electrical conductivity referenced to 25°C) between the two depths. Dashed vertical lines represent dates of ice-on and ice-off.

spring turnover does not take place immediately following ice-off, even though surface and bottom temperatures are equal. Rather spring turnover occurs some weeks to a month following ice-off, typically on a day with high wind speeds (Fig. 3C).

Analytical solution

From our analytical approach, we found that a salinity (S_{crit}) of 1.4 g kg^{-1} in Mendota and 1.3 g kg^{-1} in Monona,

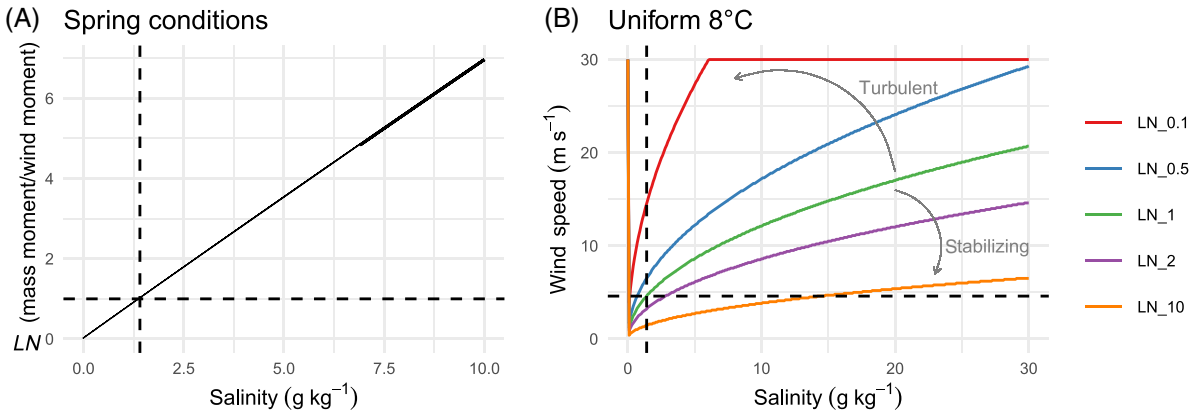

Fig 4. Analytical solution of lake water column stability under increased salt loads during spring conditions for Lake Mendota. (**A**): Lake number vs. salinity added below the center of volume. A balance of stabilizing to mixing forces, $LN = 1$, is reached with a salt content of 1.4 g kg^{-1}. (**B**) Wind speed vs. salinity content added below the center of volume. Response curves are logarithmic with low increase of stability by adding more salt under high wind speeds. Note that the horizontal and vertical dashes lines correspond to $LN = 1$ on the left, and to the critical salinity threshold and the corresponding wind speed on the right.

added below the center of volume depth, would prevent the lakes from mixing in spring. This hypothetical salt gradient would result in a density difference ($\Delta\rho$) of 1.1 kg m^{-3} between the top and bottom layers of the lake, which is unlikely under current conditions. Hypothetical salt increases resulted in a linear response of the lake number *LN* in both lake sites (Fig. 4A, Fig. S2A). Assuming a uniform water temperature distribution of 8°C, the relationship between salinity and wind speed regarding the Lake Number is represented by a logarithmic growth (Fig. 4B, Fig. S2B). Here, stabilizing conditions, $LN > 1$, occur with high salt loads under low wind speeds and vice versa for turbulent conditions, $LN < 1$. For example, to reach stabilizing conditions in the water column with 10 m s^{-1} winds an additional salt input of more than 5 g kg^{-1} is required.

Numerical solution

The average model ensemble output outperformed the fits of the individual models in both lake sites when calibrated to observed water temperature (Table S3). Simstrat had a better fit than either GLM and GOTM, and the fit metrics from all calibrations were similar to other lake modeling studies (Arhonditsis and Brett 2004; Moore et al. 2021). Overall, each model replicated mixing and heat transport dynamics of both lakes (shown for 2013–2014 in Figs. S3-S5). Calibrated parameter values (Table S2) are similar to Moore et al. (2021).

In both lakes, increasing the winter-to-spring salt load resulted in an increase in density differences throughout the year with pronounced density gradients in winter (inverse stratification under ice) and summer (summer stratification) (Fig. 5A). The theoretical density gradient threshold from the analytical approach, $\Delta\rho > 1.1$ kg m^{-3}, was only breached in the 10 g kg^{-1} salt load scenario in Lake Monona. Ice duration became slightly shorter with increased salt loads (Fig. 5B). Spring mixing usually occurred between end of March and late April in both lakes (Fig. 5C). Here, increased salt loads slightly delayed spring turnover. In the most extreme cases, salt loads of over 4.5 g kg^{-1} prevented spring mixing entirely, making fall turnover the first full mixing event of the year. With salt loads of 10 g kg^{-1}, the first mixing day of the year was sometimes in November or December. Lake water column stability during spring increased with increased external salt loads (Fig. 5D), and summer stratification durations also increased with salt loads (Fig. 5E).

Discussion

The timing and in extreme cases the occurrence of spring turnover is threatened by winter salinization in north temperate lakes. Observational data revealed that Lake Mendota and Monona currently experience different winter salinity conditions. An EC (salinity) gradient between the surface and bottom waters is slow to establish in Lake Mendota, but sets up immediately following ice-on in Lake Monona. This is likely driven by different basin morphology and inflow dynamics. Lake Monona also has higher concentrations of salt in the hypolimnion, which appears to delay spring mixing. In spring 2020, chloride at 20 m depth in Lake Monona was >200 mg L^{-1}, a concentration similar to those seen in lakes that experience salinity-induced monomixis (Bubeck and Burton 1989; Sibert et al. 2015). Note that with only two measurements of water column EC, we only recorded when the water column completely mixed and could not evaluate the gradual erosion of the vertical density gradient by wind shear during the time between ice-off and fully mixed conditions (Boehrer et al. 2014).

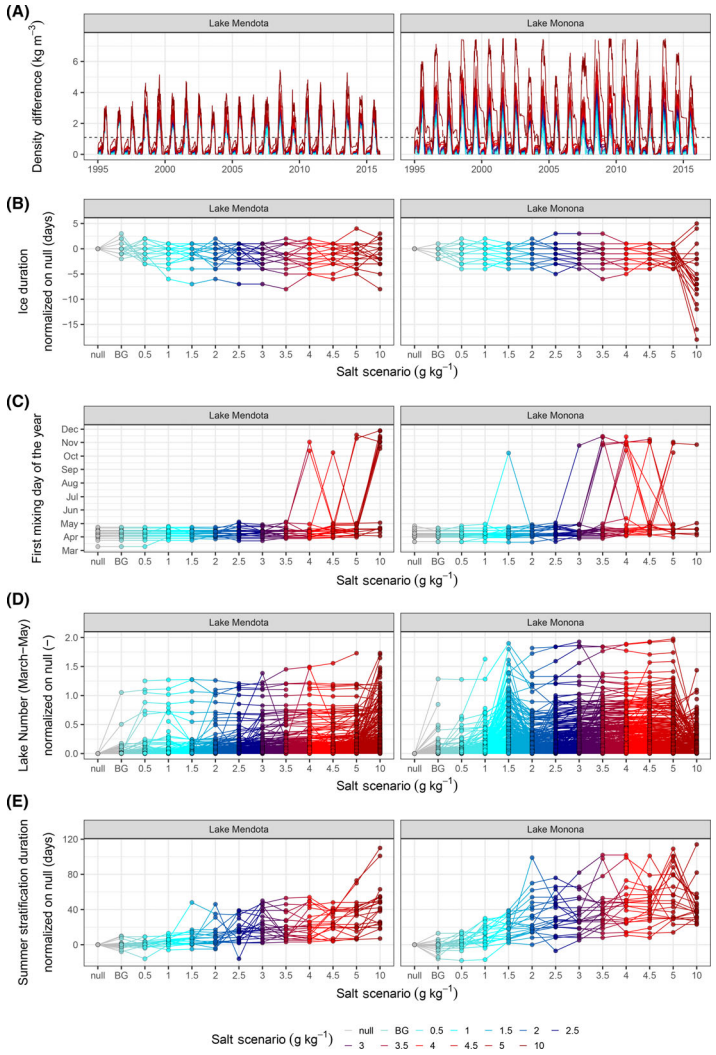

Fig 5. Average ensemble model response to the salt scenarios for Lake Mendota and Lake Monona. Note that the dots in sub-figures *B*, *C*, *D* and *E* represent individual years from 1995 to 2015. (**A**) Time series of water density differences between 20 and 2 m depth. The dashed horizontal line represents the critical gradient $\Delta\rho > 1.1$ kg m^{-3} that would theoretically prevent spring turnover (derived from analytical approach). (**B**) Ice duration normalized on null scenario for each salt load scenario. (**C**) First mixing day of the year for each salt load scenario. (**D**) Lake Numbers from March to May normalized on null scenario for each salt load scenario. (**E**) Summer stratification duration normalized on null scenario for each salt load scenario.

Our analytical model predicts that if bottom water salinity approaches 1.3 g kg^{-1}, spring mixing will be inhibited. The numerical models suggest that winter runoff with a salinity of >4 g kg^{-1} would be required to prevent spring mixing, and shift the lakes to a monomictic regime with only with only a stratified period during summer. The hypothetical bottom layer salinity threshold quantified by our analytical approach was not reached in any modeling scenario. This suggests that under field conditions the entrainment of high salt loads into the water column causes a dilution that prevents a highly localized accumulation of salt in the deep-water layers. The independent numerical models projected multiple entrainment scenarios, for example, GLM simulated entrainment of salt into the deep-water layers, which resulted in strong vertical density gradients (Fig. S3), whereas GOTM projected a near-surface entrainment of the salt loads, and a more isohaline distribution of salt in the water column (Fig. S4). As our prior knowledge of field entrainment conditions is highly uncertain, applying an ensemble approach gave us the opportunity to simulate multiple salt load scenario realizations (Fig. S3-S5). By discussing the response of the ensemble mean, we are only providing an estimation of the true value of an array of potential effects on mixing by salinization. Future work should focus verifying which hydrodynamic model best represents inflow entrainment conditions in these lakes, and at which intrusion depths the salt density currents entrain into Lake Mendota and Lake Monona (i.e., Wells and

Nadarajah 2009). Our ensemble modeling has highlighted that the ensemble average can outperform individual lake models, which is in agreement with modeling studies by Trolle et al. (2014), Kobler and Schmid (2019) and Moore et al. (2021). Nonetheless, it needs to be noted that the ensemble average can not necessarily be used for a more reliable assessment of the system.

In a dimictic lake, the two stratification periods – winter ice-covered inverse stratification and summer stratification – will be affected differently from increased external salt loads. In the winter, ice-covered periods may slightly decrease, and the spring water column will be more stable as expressed by high Lake Numbers (Fig. 5D). In the summer, the water column will be more stable and stratification duration will increase under high salt load conditions. Increased stability during both stratification periods will limit vertical transport in the water column, with ecosystem ramifications such as increased hypolimnetic oxygen depletion (Foley et al. 2012; Biddanda et al. 2018; Ladwig et al. 2021*a*), decreased habitat for fish species (Magee et al. 2018, 2019) and decreased entrainment of nutrients across the thermocline (Soranno et al. 1997).

Although Lake Mendota and Monona are receiving only a fraction of the salt loads seen in the more extreme examples of Irondequoit Bay, Wood Lake or Traunsee (Bubeck and Burton 1989; Sibert et al. 2015; Ficker et al. 2018), their long-term concentrations of chloride have been increasing since the 1940s. In Lake Monona, it appears that winter salt accumulation in the hypolimnion may already be delaying spring mixing. While we do not expect that these two lakes will reach the analytical salinity threshold of over 1.3 g kg^{-1}, which would inhibit spring turnover, anytime in the near future, the long-term trend of salt accumulation is worrisome. In the case of Lake Mendota and Monona, as well as many other similar lakes, the use of road salts should be reduced to prevent unwanted changes in the mixing regimes of urban lakes.

References

Arhonditsis, G. B., and M. T. Brett. 2004. Evaluation of the current state of mechanistic aquatic biogeochemical modeling. Mar. Ecol. Prog. Ser. **271**: 13–26. doi: 10.3354/meps271013

Biddanda, B. A., A. D. Weinke, S. T. Kendall, L. C. Gereaux, T. M. Holcomb, M. J. Snider, D. K. Dila, S. A. Long, C. VandenBerg, K. Knapp, D. J. Koopmans, K. Thompson, J. H. Vail, M. E. Ogdahl, Q. Liu, T. H. Johengen, E. J. Anderson, and S. A. Ruberg. 2018. Chronicles of hypoxia: Time-series buoy observations reveal annually recurring seasonal basin-wide hypoxia in Muskegon Lake – A Great Lakes estuary. J. Great Lakes Res. **44**: 219–229. doi: 10.1016/j.jglr.2017.12.008

Boehrer, B., and M. Schultze. 2008. Stratification of lakes. Rev. Geophys. **46**: RG2005. doi: 10.1029/2006RG000210

Boehrer, B., U. Kiwel, K. Rahn, and M. Schultze. 2014. Chemocline erosion and its conservation by freshwater introduction to meromictic salt lakes. Limnologica **44**: 81–89. doi: 10.1016/j.limno.2013.08.003

Bubeck, R. C., and R. S. Burton. 1989 Changes in chloride concentrations, mixing patterns, and stratification characteristics of Irondequoit Bay, Monroe County, New York, after decreased use of road-deicing salts, 1974-1984. *Tech. Rep. 87-4223*, U.S. Geological Survey; Copies of this report may be purchased from U.S. Geological Survey Books and Open-File Reports. doi: 10.3133/wri874223. Publication Title: Water-Resources Investigations Report.

Burchard, H., K. Bolding, and M. R. Villarreal. 1999. *GOTM, a general Ocen turbulence model: Theory, implementation and test cases*. European Commission. Join Research Centre, Space Applications Institute. Tech. Rep. EUR 18745 EN.

Burchard, H., K. Bolding, W. Kühn, A. Meister, T. Neumann, and L. Umlauf. 2006. Description of a flexible and extendable physical–biogeochemical model system for the water column. J. Mar. Syst. **61**: 180–211. doi: 10.1016/j.jmarsys.2005.04.011

Corsi, S. R., D. J. Graczyk, S. W. Geis, N. L. Booth, and K. D. Richards. 2010. A fresh look at road salt: Aquatic toxicity and water-quality impacts on local, regional, and national scales. Environ. Sci. Technol. **44**: 7376–7382. doi: 10.1021/es101333u

Dugan, H., N. K. Skaff, J. P. Doubek, S. L. Bartlett, S. Burke, F. E. Krivak-Tetley, J. C. Summers, P. Hanson, and K. C. Weathers. 2020. Lakes at risk of chloride contamination. Environ. Sci. Technol. **54**: 6639–6650.

Dugan, H. A., and L. A. Rock. 2021. The slow and steady salinization of Sparkling Lake, Wisconsin. Limnol. Oceanogr. Lett.: 10191. doi: 10.1002/lol2.10191

Engelhardt, C., and G. Kirillin. 2014. Criteria for the onset and breakup of summer lake stratification based on routine temperature measurements. Fundam. Appl. Limnol./Archiv Hydrobiol. **184**: 183–194. doi: 10.1127/1863-9135/2014/0582

EPA. 1988. *Ambient water quality criteria for chloride*. US Environmental Protection Agency.

Ficker, H., M. Luger, B. Pamminger-Lahnsteiner, D. Achleitner, A. Jagsch, and H. Gassner. 2018. Diluting a salty soup: Impact of long-lasting salt pollution on a deep alpine lake (Traunsee, Austria) and the downside of recent recovery from salinization. Aquat. Sci. **81**: 7. doi: 10.1007/s00027-018-0602-3

Foley, B., I. D. Jones, S. C. Maberly, and B. Rippey. 2012. Long-term changes in oxygen depletion in a small temperate lake: Effects of climate change and eutrophication. Freshw. Biol. **57**: 278–289. doi: 10.1111/j.1365-2427.2011.02662.x

Gaudard, A., L. Råman Vinnå, F. Bärenbold, M. Schmid, and D. Bouffard. 2019. Toward an open access to high-frequency lake modeling and statistics data for scientists

and practitioners – The case of Swiss lakes using Simstrat v2.1. Geosci. Model Dev. **12**: 3955–3974. doi: 10.5194/gmd-12-3955-2019

Goudsmit, G.-H., H. Burchard, F. Peeters, and A. Wüest. 2002. Application of k- turbulence models to enclosed basins: The role of internal seiches. J. Geophys. Res.: Oceans **107**: 954. doi: 10.1029/2001JC000954

Gray, E., E. B. Mackay, J. A. Elliott, A. M. Folkard, and I. D. Jones. 2020. Wide-spread inconsistency in estimation of lake mixed depth impacts interpretation of limnological processes. Water Res. **168**: 115136. doi: 10.1016/j.watres.2019.115136

Hintz, W. D., B. M. Mattes, M. S. Schuler, D. K. Jones, A. B. Stoler, L. Lind, and R. A. Relyea. 2017. Salinization triggers a trophic cascade in experimental freshwater communities with varying food-chain length. Ecol. Appl. **27**: 833–844. doi: 10.1002/eap.1487

Hipsey, M. R., L. C. Bruce, C. Boon, B. Busch, C. C. Carey, D. P. Hamilton, P. C. Hanson, J. S. Read, E. de Sousa, M. Weber, and L. A. Winslow. 2019. A General Lake Model (GLM 3.0) for linking with high-frequency sensor data from the Global Lake Ecological Observatory Network (GLEON). Geosci. Model Dev. **12**: 473–523. doi: 10.5194/gmd-12-473-2019

Idso, S. B. 1973. On the concept of lake stability. Limnol. Oceanogr. **18**: 681–683. doi: 10.4319/lo.1973.18.4.0681

Imberger, J., and J. C. Patterson. 1989. Physical limnology, p. 303–475. *Advances in applied mechanics*, V. **27**. Elsevier. doi: 10.1016/S0065-2156(08)70199-6

Kelly, V. R., S. E. G. Findlay, W. H. Schlesinger, K. Menking, and A. M. Chatrchyan. 2010. Road salt: Moving toward the solution. The Cary Institute of Ecosystem Studies. Special Report. 1–16.

Kobler, U. G., and M. Schmid. 2019. Ensemble modelling of ice cover for a reservoir affected by pumped-storage operation and climate change. Hydrol. Process. **33**: 2676–2690. doi: 10.1002/hyp.13519

Koretsky, C. M., A. MacLeod, R. J. Sibert, and C. Snyder. 2012. Redox stratification and salinization of three Kettle Lakes in Southwest Michigan, USA. Water Air Soil Pollut. **223**: 1415–1427. doi: 10.1007/s11270-011-0954-y

Ladwig, R., P. C. Hanson, H. A. Dugan, C. C. Carey, Y. Zhang, L. Shu, C. J. Duffy, and K. M. Cobourn. 2021*a*. Lake thermal structure drives inter-annual variability in summer anoxia dynamics in a eutrophic lake over 37 years. Hydrol. Earth Syst. Sci. **25**: 1009–1032. doi: https://doi.org/10.5194/hess-25-1009-2021

Ladwig, R., L. A. Rock, and H. Dugan. 2021*b*. Dataset: Impact of salinization on lake stratification and spring mixing v1.0 L&O Letters. *Zenodo*. doi: 10.5281/zenodo.5504319

Lindenschmidt, K.-E., and I. Chorus. 1998. The effect of water column mixing on phytoplankton succession, diversity and similarity. J. Plankton Res. **20**: 1927–1951. doi: 10.1093/plankt/20.10.1927

Magee, M. R., P. B. McIntyre, and C. H. Wu. 2018. Modeling oxythermal stress for cool-water fishes in lakes using a cumulative dosage approach. Can. J. Fish. Aquat. Sci. **75**: 1303–1312. doi: 10.1139/cjfas-2017-0260

Magee, M. R., P. B. McIntyre, P. C. Hanson, and C. H. Wu. 2019. Drivers and management implications of long-term Cisco oxythermal habitat decline in Lake Mendota, WI. Environ. Manag. **63**: 396–407. doi: 10.1007/s00267-018-01134-7

Magnuson, J., S. Carpenter & E. Stanley. 2020. North Temperate Lakes LTER: Physical Limnology of Primary Study Lakes 1981 – current ver 27.

Millero, F. J., and A. Poisson. 1981. International one-atmosphere equation of state of seawater. Deep Sea Res. Part A. Oceanographic Research Papers **28**: 625–629. doi: 10.1016/0198-0149(81)90122-9

Moore, T. N., J. P. Mesman, R. Ladwig, J. Feldbauer, F. Olsson, R. M. Pilla, T. Shatwell, J. J. Venkiteswaran, A. D. Delany, H. Dugan, K. C. Rose, and J. S. Read. 2021. LakeEnsemblR: An R package that facilitates ensemble modelling of lakes. Environ. Model. Software **143**: 1–14. doi: 10.1016/j.envsoft.2021.105101

Novotny, E., A. Sander, O. Mohseni, and H. G. Stefan. 2008. A Salt (Chloride) Balance for the Minneapolis/St. Paul Metropolitan Area Environment. *St. Anthony Falls Project Report*, **29**.

NTL-LTER. 2020. North Temperate Lakes LTER: Secchi disk depth; other Auxiliary Base crew sample data 1981 - current. Environmental Data Initiative. doi: 10.6073/pasta/c0b0b52c4c41446b76e14662f9a9a0ce.

Pesacreta, G. J., and J. C. Makarewicz. 1982. Meromixis in Ides cove, N.Y.: Causes and recovery. J. Freshwater Ecol. **1**: 467–481. doi: 10.1080/02705060.1982.9664066

Qu, Y., and C. J. Duffy. 2007. A semidiscrete finite volume formulation for multiprocess watershed simulation. Water Res. Res. **43**: 5752. doi: 10.1029/2006WR005752

Read, J. S., D. P. Hamilton, I. D. Jones, K. Muraoka, L. A. Winslow, R. Kroiss, C. H. Wu, and E. Gaiser. 2011. Derivation of lake mixing and stratification indices from high-resolution lake buoy data. Environ. Model. Software **26**: 1325–1336. doi: 10.1016/j.envsoft.2011.05.006

Richards, R. P., D. B. Baker, J. P. Crumrine, and A. M. Stearns. 2010. Unusually large loads in 2007 from the Maumee and Sandusky Rivers, tributaries to Lake Erie. J. Soil Water Conserv. **65**: 450–462. doi: 10.2489/jswc.65.6.450

Robertson, D. M., and J. Imberger. 1994. Lake number, a quantitative indicator of mixing used to estimate changes in dissolved oxygen. Int. Revue gesamten Hydrobiol. Hydrogr. **79**: 159–176. doi: 10.1002/iroh.19940790202

Rock, L. A., and H. A. Dugan . 2021. Chloride Concentrations, Conductivity, and Water Temperature Data from Lake Mendota and Lake Monona Madison, WI: December 2019 – April 2021 ver 1.

Sibert, R. J., C. M. Koretsky, and D. A. Wyman. 2015. Cultural meromixis: Effects of road salt on the chemical stratification of an urban kettle lake. Chem. Geol. **395**: 126–137. doi: 10.1016/j.chemgeo.2014.12.010

Soranno, P. A., S. R. Carpenter, and R. C. Lathrop. 1997. Internal phosphorus loading in Lake Mendota: Response to external loads and weather. Can. J. Fish. Aquat. Sci. **54**: 1883–1893. doi: 10.1139/f97-095

Stets, E., C. Lee, D. Lytle, and M. Shock. 2017. Increasing chloride in rivers of the conterminous U.S. and linkages to potential corrosivity and lead action level exceedances in drinking water. Sci. Total Environ.: 119. **613-614**: 1498–1509. doi: 10.1016/J.SCITOTENV.2017.07.119

Straile, D., K. Jöhnk, and R. Henno. 2003. Complex effects of winter warming on the physicochemical characteristics of a deep lake. Limnol. Oceanogr. **48**: 1432–1438. doi: 10.4319/lo.2003.48.4.1432

Trolle, D., J. A. Elliott, W. M. Mooij, J. H. Janse, K. Bolding, D. P. Hamilton, and E. Jeppesen. 2014. Advancing projections of phytoplankton responses to climate change through ensemble modelling. Environ. Model. Software **61**: 371–379. doi: 10.1016/j.envsoft.2014.01.032

Van Meter, R. J., and C. M. Swan. 2014. Road salts as environmental constraints in urban pond food webs. PloS One **9**: e90168. doi: 10.1371/journal.pone.0090168

Wells, M., and P. Nadarajah. 2009. The intrusion depth of density currents flowing into stratified water bodies. J. Phys. Oceanogr. **39**: 1935–1947. doi: 10.1175/2009JPO4022.1

Wilson, H. L., A. I. Ayala, I. D. Jones, A. Rolston, D. Pierson, E. de Eyto, H.-P. Grossart, M.-E. Perga, R. I. Woolway, and E. Jennings. 2020. Variability in epilimnion depth estimations in lakes. Hydrol. Earth Syst. Sci. **24**: 5559–5577. doi: 10.5194/hess-24-5559-2020

Xia, Y., K. Mitchell, M. Ek, J. Sheffield, B. Cosgrove, E. Wood, L. Luo, C. Alonge, H. Wei, J. Meng, B. Livneh, D. Lettenmaier, V. Koren, Q. Duan, K. Mo, Y. Fan, and D. Mocko. 2012. Continental-scale water and energy flux analysis and validation for the North American Land Data Assimilation System project phase 2 (NLDAS-2): 1. Intercomparison and application of model products. J. Geophys. Res.: Atmos. **117**: 27. doi: 10.1029/2011JD016048

Acknowledgments

We are very thankful to the international network for early career researchers in aquatic ecosystem modeling, AEMON-J, for developing the `LakeEnsemblR`-package. Further, we are thankful to Mark Gahler for helping with the design and deployment of the under-ice buoys. Long-term chloride data were obtained from the North Temperate Lakes Long-Term Ecological Research program (NSF DEB-1440297 and DEB-2025982), the City of Madison, and the Wisconsin Department of Natural Resources. We are also thankful to two anonymous reviewers whose comments helped to improve and clarify this manuscript. The project was funded through an United States National Science Foundation (NSF) ABI development grant (DBI 1759865).

Submitted 11 June 2021
Revised 24 August 2021
Accepted 12 September 2021